COMPARISON OF THE HIGH CURRENT BOOST CONVERTERS GENERATED WITH THREE-STATE SWITCHING CELL

Grover Victor Torrico-Bascopé

Eltek Valere
Dept. of Research and Development
Hammarbacken 4A, 4tr. 191 24, Sollentuna, Stockholm, Sweden - www.eltekvalere.com
grover.torrico@eltekvalere.com quillagro@hotmail.com

Ivo Barbi

Power Electronics Institute - INEP
Dept. of Electrical Engineering
Federal University of Santa Catarina - UFSC
P.O. Box 5119 - 88040-970 - Florianópolis - SC -Brazil
www.inep.ufsc.br ivobarbi@inep.ufsc.br

***Abstract* – This work presents a comparison of non-isolated DC-DC PWM boost type converters obtained using three-state switching cells (3SSCs). The mentioned cells are composed by two controlled switches, diodes, one autotransformer, and one simple or coupled inductor. The main advantages of these converters compared to the classical converters, are: low conduction losses, reduced current ripple in the input and the output, double switching frequency operation of the reactive elements which permits weight and volume reduction. Due to such characteristics, the boost family converters remains gaining more importance in low input voltage and high current applications, mainly in photovoltaic, fuel cell, wind, and DC power distributed systems. The converters are analyzed for two operation duty cycles (D≤0.5 and D≥0.5). Thus, the theoretical analysis, comparative analysis, and experimental results obtained from prototypes are presented.**

***Keywords* – boost converters, step-up converter, three-state switching cell, renewable energy applications.**

I. INTRODUCTION

Today the photovoltaic, fuel cell, wind, and DC power distribution systems are continuously growing into the industrial applications. Different Power Architectures (DPA) has been used to achieve suitable output voltages and loads. That means that high density and high efficient power systems are required to fulfill the specifications and standards. For the designer it is very difficult to select which topology of converters is suitable for a particular application given the specifications of the system. Some of the more common characteristics, which should be compared, are: component stress levels, circuit complexity, number of passive and active components, efficiency of the power conversion, weight and volume of the converter, required control loops, input to output dynamics transfer functions, input and output filtering requirements (EMI), energy storage capability in reactive elements, effect of the non-ideal components on desired performance, manufacturing and place, maintainability, packaging, cost, etc. In order to simplify the problem of selection, it is better to arrange the circuits into groups, with common properties and start to consider the differences among circuit variations in detail in order to achieve an optimum solution.

Pulse-width modulated (PWM) converters are currently used in the majority of DC-DC conversion applications. Widespread applications of DC-DC converters include power supplies for a countless variety of electronic systems, telecommunications energy systems, renewable energy systems, fuel cell systems, DC motor drivers and satellite energy systems.

A family of DC-DC non-isolated PWM converters using the **Three-State Switching Cell** (**3SSC**) has been presented in [1]. Those topologies is being utilized at the industry in different types of applications. For instance, the converter generated with cell "B" is mainly being utilized as a pre-regulator to obtain unitary power factor and low THD with universal AC input [3, 4]. This converter also has been compared with the conventional boost [5], presenting a better performance. The boost family topologies may be applied at high density power distributed architecture systems to guarantee controlled DC bus voltage and non-pulsed current avoiding input filter installations. Those converters are also suitable to UPS systems where is necessary to boost the voltage from the batteries to the desired dc-link of the input of the inverter.

In this paper, three DC-DC boost converter topologies applying **3SSCs** are compared. In Fig. 1 the circuits are obtained using cells B, D and E presented in [1]. Those are controlled by pulse width modulation PWM. The proposed converters are capable of operating at high power (>1kW) and high frequency applications. They present reduced input and output current ripple which permit smaller filter capacitor utilization. The qualitative and quantitative analysis and experimental tests have been done at [2]. In this paper, a comparative analysis of the mentioned converters above is presented. This comparison is based on some important parameters, as component stress, converter complexity and efficiency.

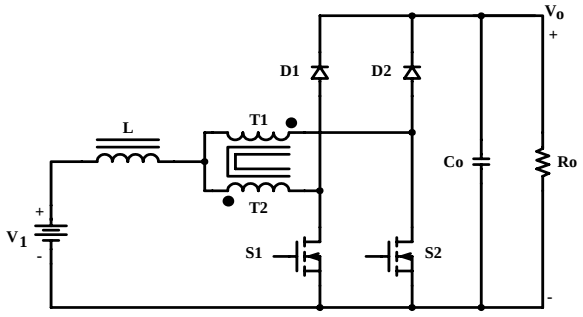

(a) Converter 1 using cell "B".

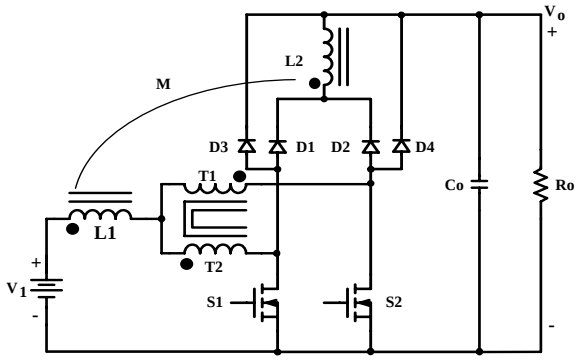

(b) Converter 2 using Cell "D".

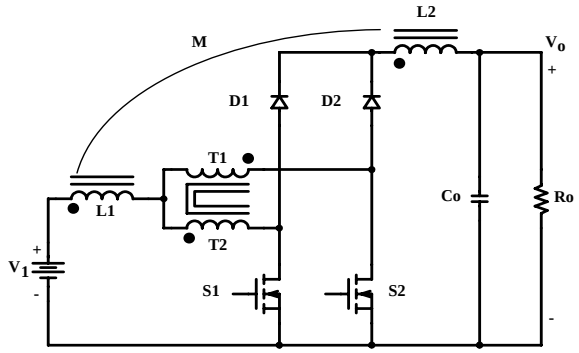

(c) Converter 3 using cell "E"

Fig.1 - Non-Isolated boost converters using 3SSCs.

II. DESCRIPTION OF THE CONVERTERS

To analyze the three converters, the following considerations are assumed:

- The semiconductors are ideals,
- The turn-ratio of the auto-transformer and the flyback inductor is unitary,
- The input and output voltages are DC voltage sources,
- The control of the switches is assumed to be symmetrical and phase shifted 180 degrees between them.

Converter 1: is based on the cell "B" obtained from the Current-Fed Push-Pull converter presented in [1]. With an appropriate gate signals for the switches, the converter can work in Non-overlapping mode (0<D<0.5) and in overlapping mode (0.5<D<1), where D is the duty cycle of the switches. At both cases the input current that goes through the input inductor is divided by the windings of the autotransformer. The theoretical analysis, including operation principle, and main waveforms for this converter was presented in [1, 2].

Fig. 2 shows the ideal voltage gain as a function of the duty cycle. The output characteristic of the converter is shown at Fig. 3 for both operation modes.

0<D<0.5	0.5<D<1
$\frac{V_o}{V_i}=\frac{1}{1-D}$	$\frac{V_o}{V_i}=\frac{1}{1-D}$

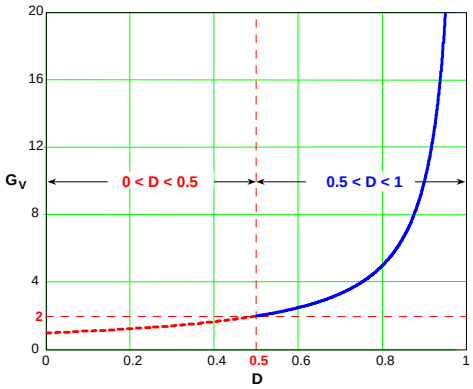

Fig. 2. Voltage gain as a function of the duty cycle (D).

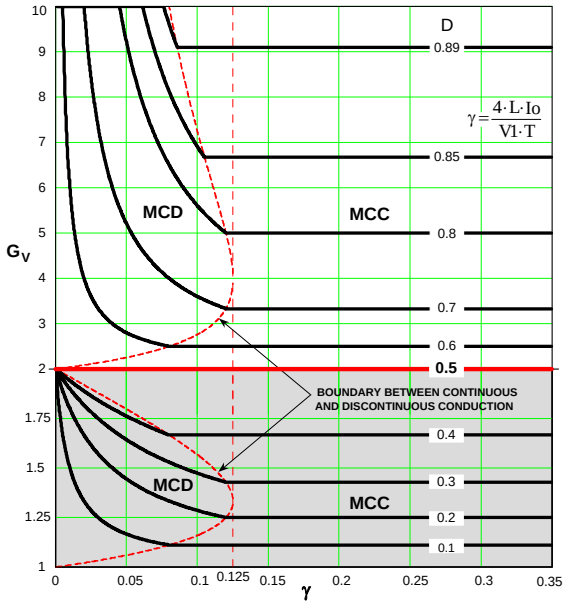

Fig. 3. Output characteristic of the converter.

Converter 2: is based on the cell "D" obtained from the Weinberg modified converter [1]. Similar to the previous converter, it can work in Non-overlapping mode (0<D<0.5) and overlapping mode (0.5<D<1). Compared to the cell B, two diodes and one output inductor, which is coupled with the input inductor are added in cell D. The inductor acts as a flyback transformer in this circuit. When the converter works with the duty cycle lower than 50%, the reverse recovery current of the diode is controlled by the leakage inductance of the transformer. The complete theoretical analysis, including operation principle and main waveforms for this converter is presented in [2]. Fig. 4 and Fig. 5 show for both operation modes the ideal voltage gain and the output characteristic of the converter.

0<D<0.5	0.5<D<1
$\frac{V_o}{V_i} = 1 - 2 \cdot D$	$\frac{V_o}{V_i} = \frac{2 \cdot D + 1}{2 \cdot (1 - D)}$

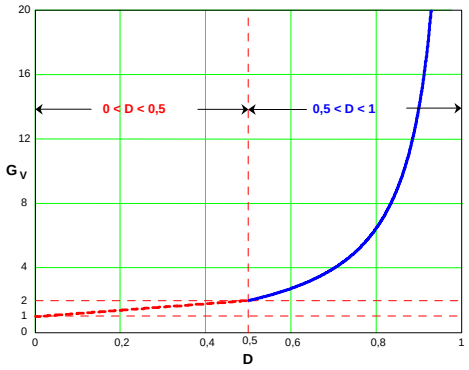

Fig. 4. Voltage gain as a function of the duty cycle (D).

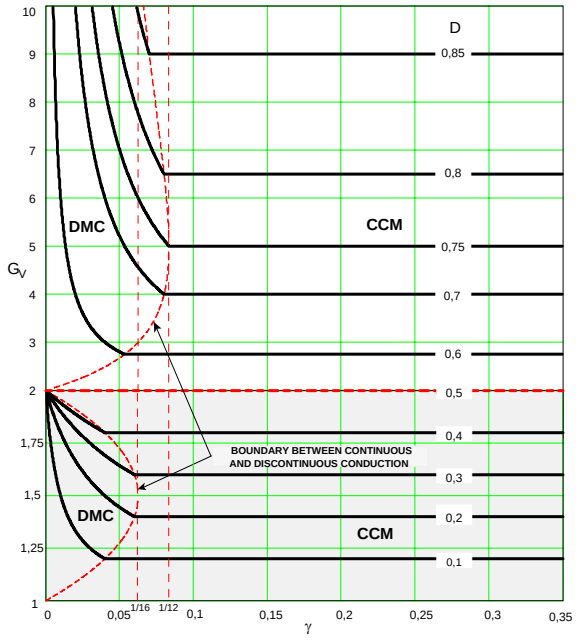

Fig. 5. Output characteristic of the converter.

Converter 3: is based on the cell "E" obtained from the Flyback Current-Fed Push-Pull Converter [1]. It is capable of operating in Non-overlapping mode (0<D<0.5) and overlapping mode (0.5<D<1). Compared to the cell D, in cell E two diodes are removed. This inductor coupling feature gives a non-pulsated current in the input and the output. The complete analysis including operation principle, main waveforms, and theoretical analysis for this converter is also presented in [2]. In Fig. 6 and Fig. 7 are shown the ideal voltage gain and the output characteristic of the converter.

0<D<0.5	0.5<D<1
$\frac{V_o}{V_i} = \frac{3 + 2 \cdot D}{3 - 2 \cdot D}$	$\frac{V_o}{V_i} = \frac{2 \cdot D + 1}{2 \cdot (1 - D)}$

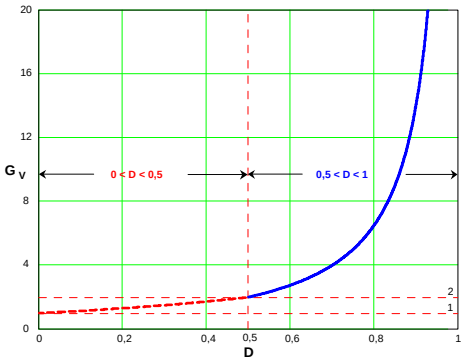

Fig. 6. Voltage gain as a function of the duty cycle (D).

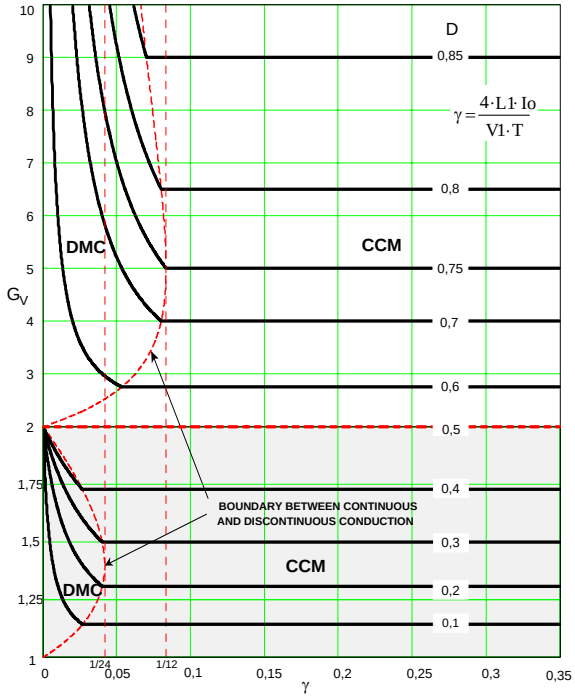

Fig. 7. Output characteristic of the converter.

III. COMPARATIVE ANALYSIS OF THE CONVERTERS

Based on the specifications parameters of the converter (see Table I), the converters were designed and assembled. For the inductances and capacitances indicated, the voltage and current stresses on the main components of the three converters are shown in Table II. Using these values, a comparative analysis between them can be made. Other comparative criterion is strongly connected to the application of the converter. For example, if a certain application has very tight EMI requirements in the input, then a converter with a non-pulsating input current must be chosen to reduce the cost and volume of the input filter. The same criterion must be used when EMI requirements are necessary in the output of the converter.

Another important parameter is the current through the main switches that influence the converter efficiency.

TABLE I
Specifications parameters of the converters

Duty Cycle Range	**0<D<0.5**	**0.5<D<1**
Input Voltage Vi [V]	48.00	24.00
Output Voltage Vo [V]	60.00	60.00
Output Power Po [W]	2000.00	1000.00
Switching Frequency Fs [kHz]	30.00	30.00

TABLE II

				Converter 1		**Converter 2**		**Converter 3**	
Parameters				**D<0.5**	**D>0.5**	**D<0.5**	**D>0.5**	**D<0.5**	**D>0.5**
VOLTAGE	**[V]**	PEAK	V_{S1}	60.00	60.00	60.00	56.00	72	56.00
			V_{D1}	60.00	60.00	78.00	84.00	54	84.00
			V_{D3}	-	-	60.00	24.00	-	-
CURRENT	**[A]**	PEAK	I_{S1}	22.03	21.63	35.21	30.59	26.11	30.59
			I_{D1}	22.03	21.63	17.6	20.40	26.11	20.40
			I_{D3}	-	-	35.21	0.00	-	-
			I_L	44.70	43.28	68.54	61.19	52.22	61.19
		RMS	I_{S1}	9.34	16.14	11.79	16.85	10.21	16.85
			I_{D1}	18.64	13.8	14.44	12.73	18.41	12.73
			I_{D3}	-	-	11.79	0.00	-	-
			I_C	10.21	8.34	1.08	6.82	5.96	6.82
			I_L	41.69	41.68	44.10	42.23	42.03	42.23
		AVG	I_{S1}	4.17	12.50	4.17	12.50	4.17	12.50
			I_{D1}	16.67	8.33	12.50	8.33	16.67	8.33
			I_{D3}	-	-	4.17	0.00	-	-
L_{Crit}	**[uH]**			1.60	1.50	0.80	1.00	0.50	1.00
L	**[uH]**			29.00	29.00	19.94	23.50	11.13	23.50
C	**[uF]**			277.60	185.02	26.04	132.30	154.30	132.30
E_{Lcri}	**[mJ]**			1.598	1.405	1.879	1.872	0.682	1.872

The comparative analyses are realized for continuous conduction mode (CCM) of the converters, and duty cycles lower than 50%, and higher than 50%.

a) Volume

The inductor inductance, L, of each converter is calculated using maximum current ripple as a function of the duty cycle. The critical inductance, L_{crit}, are calculated from the maximum transition point of the curves DCM and CCM as shown in Fig. 3, Fig. 5, and Fig. 7. For value of L_{crit}, the storage peak energy into the inductor can be calculated ($E_{Lcrit}=1/2L_{crit}I_{Lpk}^2$). The voltage and current values for the three converters are shown in Table II.

If we assume that the size of the inductor is proportional to the peak of the storage energy, then the inductor of the Converter 3 is lower than inductor on Converter 1 and Converter 2. So, based on the storage energy in Converter 3, it can be observed that the energy on Converter 1 and Converter 2 are 2.47 and 2.32 times higher respectively. So, the volume of these inductors is larger. On the other hand, the inductors of the Converter 2 and Converter 3 are of flyback type (two windings) which means that those could be more complex to manufacture compared to the inductor in Converter 1, which is a single winding inductor. Therefore, this is a disadvantage from the manufacturing point of view.

The autotransformers of the three converters are similar, because the rms current trough the windings and rms voltage across the winding are almost equal. This means that the volume and the weight of the three autotransformers are almost equal.

Considering that output voltage ripple is equal for each converter, the value of the capacitance of the output filter capacitor are given in table II. The capacitance of the Converter 2 is almost 10 times lower than the capacitance of the Converter 1, and 5 times lower than capacitance of the Converter 3. Usually, in a real application, the capacitors volume is defined by rms current through them and their equivalent series resistance (Resr) which will define the dynamic comportment of the control loop. In some cases, the required Hold-up time will determinate the size of those capacitors.

In this work, the number of capacitors required in each converter is based only in the rms current (capacitor EKZ800ELL391MK30S), as illustrated in Table III. From this table, it can be concluded that Converter 1 shows a large volume compared to the other two converters.

The volume of the heat-sink has a direct relation with the losses on the semiconductors (thermal resistance). From the Table IV, can we conclude that the volumes of the heat-sinks in the three converters are similar since the losses are almost equals.

b) Complexity

The level of complexity of the circuit is related directly to the number of components. Those are mainly the active devices and their corresponding controllers, the EMI filter and the manufacturing of the magnetic elements. The number of the components is shown in Table III. The three converters have a common ground in order to easily implement the control.

Converters 2 and 3 have a flyback-type inductor, which increases their complexity, but Converter 1 is much easier to manufacture, as it has a single winding inductor.

c) Efficiency

Another parameter to find the adequate topological circuit is the efficiency. Hence, with the components selected in table V, the losses are determined. The theoretical efficiency of each converter is calculated in table IV. Converter 1 presents higher efficiency compared to Converter 2 and Converter 3.

d) Cost

The cost is sometimes a parameter that will define which kind of topological circuit will be used in a specific design. It is very important for industry applications. For this reason, it is a big challenge to find a trade-off between circuits and component manufactures. This parameter has not been considered in the analysis presented here.

Furthermore, there are other parameters of comparison like weight, size of EMI-filter, non idealities of the circuit components, among others, that are not considered either.

TABLE III

	Converter 1		Converter 2		Converter 3	
Components	**D<0.5**	**D>0.5**	**D<0.5**	**D>0.5**	**D<0.5**	**D>0.5**
Switches	2	2	2	2	2	2
Diodes	2	2	4	4	2	2
Transformers	1	1	1	1	1	1
Inductors	1	1	1	1	1	1
Capacitors	7	6	1	5	4	5

TABLE IV
Losses in watts.

		Converter 1		Converter 2		Converter 3	
Components		**D<0.5**	**D>0.5**	**D<0.5**	**D>0.5**	**D<0.5**	**D>0.5**
Switches	**Con.**	1.66	4.95	2.64	5.39	1.98	5.39
	Sw	0.34	0.36	0.88	0.29	0.45	0.29
Diode D1	**Con.**	16.67	8.33	12.50	8.33	16.67	8.33
Diode D3	**Con.**	-	-	4.17	-	-	-
Transf.	**Mag.**	3.69	3.69	3.69	3.69	3.69	3.69
	Cu	2.10	1.90	2.13	2.05	2.44	2.05
Inductor	**Mag.**	0.0346	0.0346	0.0235	0.018	0.0220	0.0180
	Cu	3.96	3.96	3.87	2.81	3.53	2.81
Capacitor	**Con.**	0.1828	0.1608	0.0933	0.1395	0.1776	0.1395
Clamper	**Con.**	0.78	0.71	0.78	0.79	0.80	0.79
Total Losses		48.09	37.73	50.88	37.52	48.84	37.52
η	**[%]**	97.65	96.36	97.52	96.38	97.61	96.68

IV. EXPERIMENTAL RESULTS

Table V illustrates the list of components used in the prototypes for the estimation of losses and the experimental results.

TABLE V

Mosfets	APT10M11VLR	100V-100A
Diodes	30CPQ150	150V-30A
Transformers	E55/28/21 IP12	N_{T1}=N_{T2}=5 turns.
Inductors	E55/28/21 IP12	N_L=10 turn-N_{L1}=N_{L2}=5 turn
Capacitors	EKZ800ELL391MK30S	80V-1.5A 390uF
Controller ICs	SG3525/SG3527	35V-400mA
Heat-sink	Aluminum	1.1ºC/W
Clam. Diodes	MUR120	200V-1A
Clam. Resistor	Metal Film	33Ω/10W
Clam. Cap.	MKT Polypropylene	1uF/100V

To tests the converters, two different control circuits have been used, one for duty cycle variation between 0 and 0.5 and other for duty cycle variation between 0.5 and 1.

A. Photography of the Converters:
Fig. 8 show the circuit of Converter 1 and pictures of the three converters.

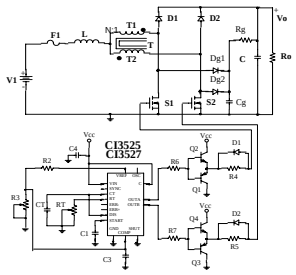

(a) Circuit tested

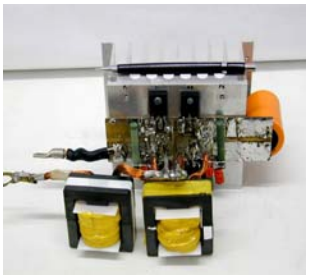

(b) Converter 1

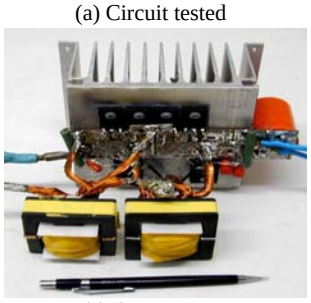

(c) Converter 2

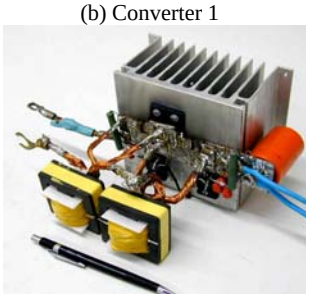

(d) Converter 3

Fig. 8. Circuit and Photography of the converters.

- Results for D≤0.5
Fig. 9.a, Fig. 9.b, and Fig. 9.c show waveforms of the Converters 1, Converter 2, and Converter 3. The waveforms description is realized from left to right. Thus, input voltage V1, inductor current IL, output voltage Vo, current before the output capacitor Ivo, and output current Io, are shown.

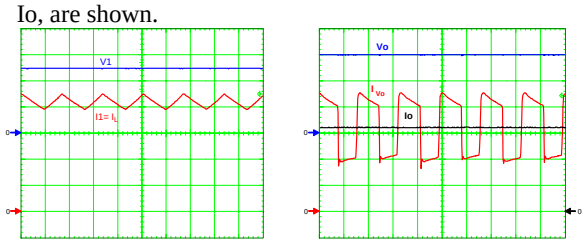

(a) Converter 1

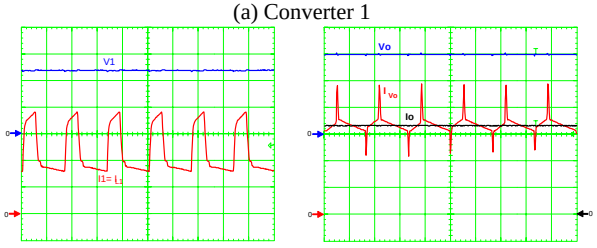

(b) Converter 2

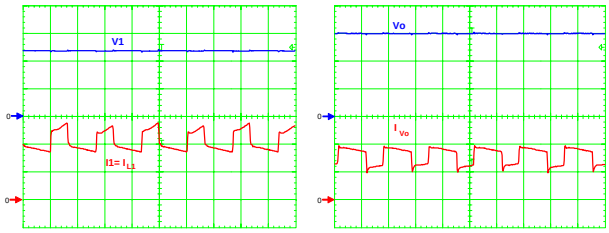

(c) Converter 3

Fig. 9. Input voltage V1; inductor current IL; output voltage Vo, current before output capacitor Ivo; and output current Io. Scale: voltage (20V/div.), current (10A/div.), time (10us/div.)

Fig. 10 shows the measurements of efficiency of the converters when the duty cycle is lower than 0.5.

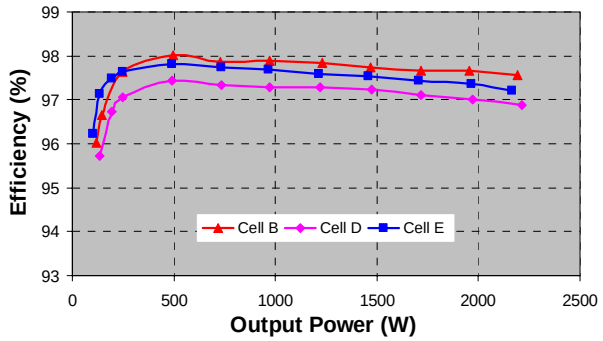

Fig. 10. Efficiency as a function of the power.

- Results for D≥0.5

The waveforms shown in Fig. 11.a, Fig. 11.b, and Fig. 11.c are similar to the ones described in Fig.9.

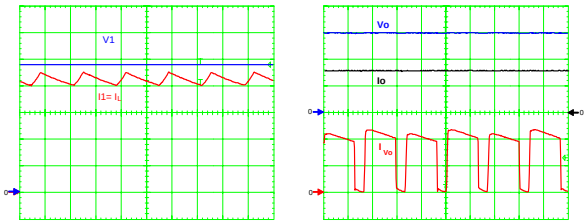

(a) Converter 1

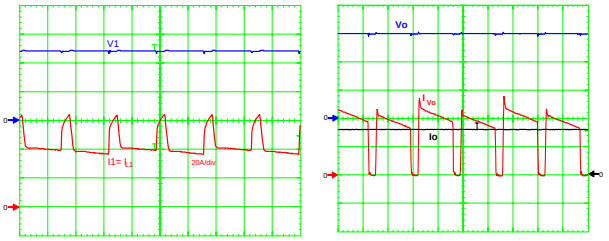

(b) Converter 2

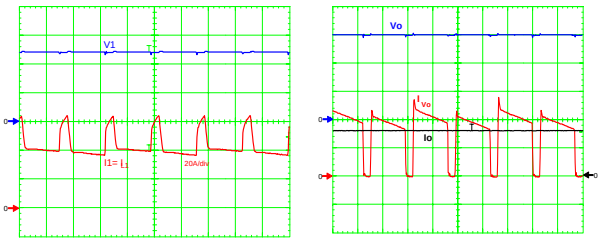

(c) Converter 3

Fig. 11. Input voltage V1; inductor current IL; output voltage Vo, current before output capacitor Ivo; and output current Io. Scale: voltage (20V/div.), current (10A/div.), time (10us/div.)

Fig. 12 shows the measurements of efficiency of the converters when the duty cycle is higher than 0.5.

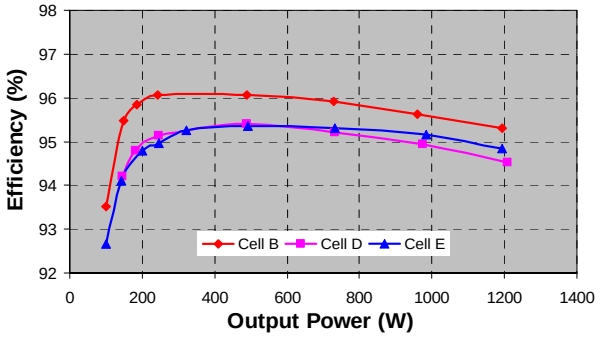

Fig. 12. Efficiency as a function of the power.

V. CONCLUSION

From the study presented in this paper, following conclusions can be drawn:

- A comparative study of three converters, based on the three-state switching cell has been presented.
- The theoretical analysis, as well as experimental results, show that the Converter 1 using cell "B", has the best efficiency and lower complexity, but presents higher volume relative the others.
- The control strategy for the three converts is simple of being implemented, such for duty cycle lower than 0.5, and for higher than 0.5.
- To illustrate if the current are pulsed or non-pulsed, in the input and the output of the converters, the mains waveforms were presented.
- The topologies presented are suitable for industrial applications, especially when low voltage and high current DC-DC conversion are required.

REFERENCES

[1] G. V. Torrico-Bascopé, and Ivo Barbi, **"***Generation of a Family of Non-Isolated DC-DC PWM Converters Using New Three-State Switching Cells"***,** IEEE PESC, 2000 Record, pp. 858-863, Galway, Ireland, 2000.

[2] G. V. Torrico-Bascopé, "*New Family of dc-to-dc PWM converters Using New Three-State Switching Cells"***,** PhD. Thesis, SC-Brazil, 2001.

[3] G. V. Torrico-Bascopé, and N. Backman, **"***Control Method and Device for a Converter Using a Three-State Switching Cell"***,** Patent: WO/2006/137744, December, 28, 2006.

[4] G. V. Torrico-Bascopé and I. Barbi "*A Single Phase PFC 3kW Converter Using Three-State Switching Cells*", in Proc. of IEEE PESC 2004, pp. 4037-4042, Aachen, Germany, 2004.

[5] C. A. Petry, and I. Barbi, "*A Comparison Between the Boost and the Double Boost Converters with Inductive Coupling"***,** COBEP 2003, pp. 51-56, Fortaleza, Ceará, Brazil, 2003.

[6] A. Weinberg, H. Boldo, P. Rueda, "*High Power, High Frequency, DC to DC Converter For Space Applications"*. IEEE PESC'92 - *Power Electronics Specialists Conference Records*, 1992. pp. 137-142.